

Phonons in Ge/Si Superlattices with Ge Quantum Dots

A. G. Milekhin^{1,*}, A. I. Nikiforov¹, O. P. Pchelyakov¹, S. Schulze², and D. R. T. Zahn²

¹ *Institute of Semiconductor Physics, Siberian Division, Russian Academy of Sciences,
pr. Akademika Lavrent'eva 13, Novosibirsk, 630090 Russia*

* e-mail: milekhin@thermo.isp.nsc.ru

² *Institut für Physik, Technische Universität Chemnitz, D-09107 Chemnitz, Germany*

Received March 7, 2001; in final form, March 20, 2001

Ge/Si superlattices containing Ge quantum dots were prepared by molecular beam epitaxy and studied by resonant Raman scattering. It is shown that these structures possess vibrational properties of both two- and zero-dimensional objects. The folded acoustic phonons observed in the low-frequency region of the spectrum (up to 15th order) are typical for planar superlattices. The acoustic phonon lines overlap with a broad emission continuum that is due to the violation of the wave-vector conservation law by the quantum dots. An analysis of the Ge and Ge–Si optical phonons indicates that the Ge quantum dots are pseudoamorphous and that mixing of the Ge and Si atoms is insignificant. The longitudinal optical phonons undergo a low-frequency shift upon increasing laser excitation energy (2.54–2.71 eV) because of the confinement effect in small-sized quantum dots, which dominate resonant Raman scattering. © 2001 MAIK “Nauka/Interperiodica”.

PACS numbers: 63.22.+m; 78.67.Hc; 78.30.Fs

In the last few years, semiconductor Ge/Si structures have been intensively studied because of their potential use in optoelectronic devices compatible with silicon technology. Their vibrational properties are well studied and understood [1–3]. It was recently demonstrated that molecular beam epitaxy allows one to prepare, under certain growth conditions, dislocation-free Ge quantum dots (QDs) of various size (8–95 nm in base and 1–7 nm in height) [4–6]. It is expected that the Ge/Si superlattices (SLs) containing Ge QDs should combine QD advantages over the Ge/Si SL and, at the same time, retain a compatibility with silicon technology. Although considerable progress has been achieved in the Ge QD growth technology, the inquiry into the optical properties of these structures is presently the subject of numerous theoretical and experimental works.

Recently, Raman scattering spectroscopy was successfully applied in studying the built-in mechanical stress and the mixing effect in Ge QDs using the frequencies of longitudinal optical (LO) Ge and Ge–Si phonons [4, 7, 8]. Transverse optical (TO) phonons are not observable in these experiments because, according to the Raman selection rules, they are inactive in the scattering geometry used. As in the case of planar Ge/Si SLs, Raman spectra of the Ge/Si SLs with QDs show lines due to the folded longitudinal acoustic (LA) phonons in the low-frequency region [8]. At the same time, the presence of QDs is expected to weaken or even remove the selection rules, because the wave-vector conservation law is no longer operative in such a structure, so that Raman scattering can involve phonons

in the “forbidden” geometry. Nevertheless, this problem has not been studied in detail so far.

This work reports the results of studying the vibrational spectra of periodic structures with Ge QDs by resonant Raman scattering. It is demonstrated that these structures possess vibrational properties that are typical of both two- and zero-dimensional objects. The observation of QD-size-selective resonant Raman scattering from the LO phonons confined in Ge QDs is reported.

Samples for investigation were grown by molecular beam epitaxy in the Stranski–Krastanov growth regime on a (001)-oriented Si substrate coated with a 20-nm-thick buffer Si layer. The growth temperature for the Si layers was 800 and 500°C, respectively, before and after applying the Ge layer. The Ge layers with QDs were grown at a temperature of 300°C. The nominal thicknesses of the Ge and Si layers were 1.4 and 37 nm, respectively. The number of repetitive Ge and Si layer pairs was 10. The structural monitoring of the QD parameters was performed by high-resolution transmission electron microscopy of the structure cross section.

The Raman experiments were carried out with a Dilor XY800 spectrometer in the backscattering geometries $z(xx)z$ and $z(xy)z$ using the excitation lines of Ar⁺, Kr⁺, and HeNe lasers in the wavelength range 676.4–457.9 nm (1.83–2.71 eV). Raman spectra in the $y'(zz)y'$ and $y'(zx')y'$ geometries were recorded at a wavelength of 514.5 nm of the Ar⁺ laser using a microscope focusing light into a spot of diameter 1 μm onto the sample cross section. The x , y , z , x' , and y' indices correspond to

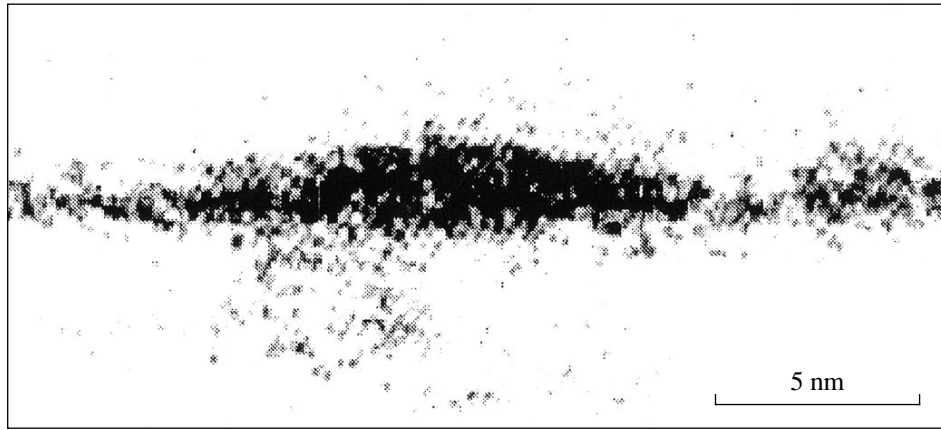


Fig. 1. High-resolution electron microscopy image of the sample. The dark area corresponds to the Ge layer with quantum dots.

the directions parallel to the $[100]$, $[010]$, $[001]$, $[\bar{1}\bar{1}0]$, and $[110]$ axes, respectively.

Figure 1 is a high-resolution electron microscopy image of the sample. The dark area corresponds to a layer with Ge QDs, and the light area corresponds to Si. One can see that the Ge QD is pyramid-shaped with a base on the order of 15 nm and a height of 2 nm. These parameters agree well with the tunneling microscopy data for samples prepared under similar growth conditions [9].

The Raman spectra recorded for different geometries are shown in Fig. 2. The low-frequency region of the $z(xx)z$ Raman spectra shows a line progression (up to the 15th order) due to folded LA phonons (FAPs) in the SL with Ge QDs. This fact is consistent with the Raman selection rules for the planar Ge/Si SLs [1]. The doublets of folded phonons are not resolved because of a small splitting (about 1 cm^{-1}) for the wave vector used in the experiment. The FAP lines overlap with a broad emission continuum with a maximum near 40 cm^{-1} . The FAP frequencies can be calculated using the dielectric continuum model [10], according to which the FAP dispersion in a periodic structure (e.g., Ge/Si) can be represented as

$$\begin{aligned} \cos(qd) &= \cos\left(\frac{\omega d_1}{v_1}\right)\cos\left(\frac{\omega d_2}{v_2}\right) \\ &- \frac{k^2 + 1}{2k} \sin\left(\frac{\omega d_1}{v_1}\right)\sin\left(\frac{\omega d_2}{v_2}\right), \end{aligned} \quad (1)$$

where $k = v_1\rho_1/v_2\rho_2$; $d = d_1 + d_2$; and d_1 and d_2 , ρ_1 and ρ_2 , and v_1 and v_2 are the thicknesses, the densities, and the sound velocities for the Ge and Si layers, respectively. The FAP dispersion calculated with parameters taken from [3] is shown in the inset in Fig. 2. The horizontal line in the inset corresponds to the wave vector used in the experiment. One can see from Fig. 2 that the agreement with the model is very good and there is no need to introduce any additional fitting parameters. The

calculated period of the structure is 37.9 nm, in compliance with the value obtained from the high-resolution microscopy experiments.

The origin of the emission continuum observed in the Stokes and anti-Stokes regions of the $z(xx)z$ spectrum can be understood using the model of interaction between electrons (holes) confined in a quantum well and acoustic phonons. The charge-carrier confinement in a quantum well, whose width fluctuates because of the insular growth regime, breaks the translational symmetry and renders the whole acoustic branch Raman-active [11, 12]. The corresponding resonant Raman intensity is expressed as $q_z|M_{qz}|^2$, where q_z is the wave vector of a phonon propagating along the z axis and M_{qz} is the electron-phonon matrix element given by

$$M_{qz} = \int e^{iq_z z} |\varphi(z)|^2 dz. \quad (2)$$

Here, the wave function $\varphi(z)$ of the localized hole is taken in the form $\varphi(z) = a^{1/2}e^{-|z|/a}$, where a is the average thickness of the layer containing Ge QDs. This model was employed to calculate the Raman spectrum for a Ge layer thickness of 1.2 nm (Fig. 2, dotted line). The interaction between the neighboring layers with QDs was assumed to be negligible. One can see from Fig. 2 that this model adequately describes the experiment and that the Ge layer thickness is in agreement with its nominal value specified in the structure growth (1.4 nm). It is notable that the band maximum and shape strongly depend on the form of wave function. For this reason, the quantitative estimates should be done with the wave functions that are most appropriate to the geometry of the structures under study.

Let us now consider the optical phonon frequency range.

In the SLs containing Ge QDs, the optical phonons are split into two branches whose wave vectors are directed either along or perpendicular to the (001) direction: LO phonons and doubly degenerate TO phonons, respectively. According to the Raman selec-

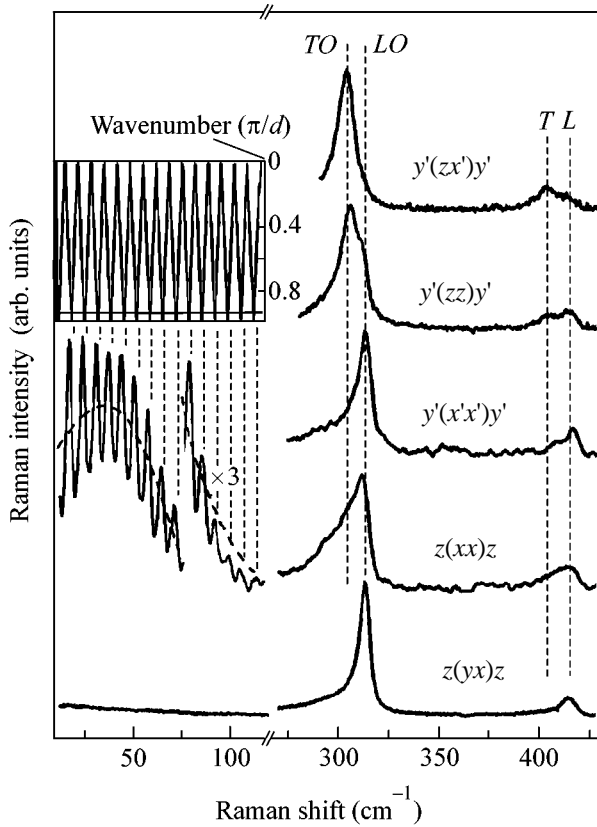


Fig. 2. Raman spectra recorded for the sample in different geometries. Inset: the calculated dispersion of acoustic phonons in the structure. The horizontal line corresponds to the wave vector used in the experiment.

tion rules, the *LO* phonons in the planar Ge/Si SLs grown on a (001) Si substrate should be observable in the Raman spectra for the $z(yx)z$ and $y'(x'x')y'$ scattering geometries, while the *TO* phonons are active in the $y'(zx')y'$ geometry [1]. The selection rules for Raman scattering in the SL containing Ge QDs are expected to weaken because of symmetry lowering. As a result, the “forbidden” vibrational modes become Raman-active in the structures with QDs. Indeed, as in the case of planar Ge/Si SLs, the experimental spectra of the structures with QDs (Fig. 2) show *LO* (315 cm^{-1}) and *TO* (308 cm^{-1}) phonons in the $z(yx)z$, $y'(x'x')y'$ and $y'(zx')y'$ geometries, respectively. Strong lines corresponding to the *LO* or to the *LO* and *TO* phonons are additionally observed in the forbidden $z(xx)z$ and $y'(zz)y'$ geometries, respectively, indicating the weakening of the Raman selection rules in the SL containing Ge QDs. Weak Raman lines observed at 405 and 417 cm^{-1} are caused by the transverse and longitudinal Ge–Si interface phonons labeled, respectively, *T* and *L* in Fig. 2.

A high-frequency shift of the *LO* and *TO* Ge phonons in QD relative to their bulk frequency (300 cm^{-1}) points to the presence of a strong mechanical stress in the QD. The calculation using the known dependence of phonon frequencies on mechanical

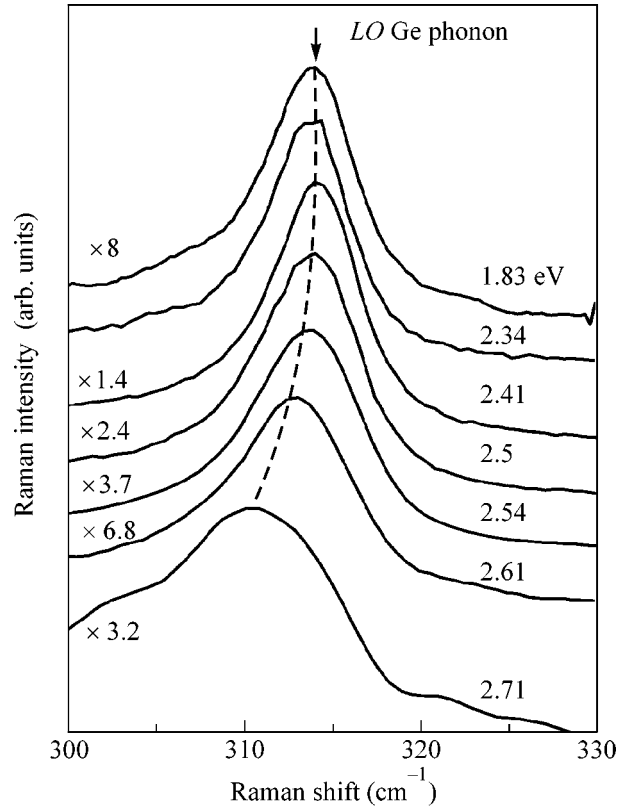


Fig. 3. The Raman frequency and intensity of *LO* phonons for different laser excitation energies.

stress [13] suggests that the Ge QDs are biaxially compressed to an extent of about 3.6% [8]. The *TO* and *LO* frequencies in this state are equal, respectively, to 310.6 and 315 cm^{-1} . A good coincidence with the experimental frequencies of optical phonons, as well as the small width of the corresponding lines (about 6 cm^{-1} at a half height), is evidence that the Ge QDs are unrelaxed and that there is no atomic mixing at the Ge–Si interface. A large experimental value of the *LO*–*TO* splitting is explained by the fact that the *LO* and *TO* phonons are characterized by different degrees of confinement in the Ge/Si structures. Indeed, only the *TO* Ge phonons are confined in the Ge/Si SL, because their frequencies do not overlap with the frequencies of optical and acoustic Si phonons. The longitudinal optical phonons in the Ge layers are quasi-localized because the Ge *LO* and Si *LA* bands overlap.

The observed *L*–*T* splitting fits the data in [2] and is explained by the fact that the atomic clusters contributing to the *L* and *T* vibrations have different character at the Ge/Si interface.

Whereas the acoustic phonons in the Ge/Si SL with QDs are satisfactorily described by the two-dimensional model, the behavior of optical phonons in the Raman spectra recorded at different laser excitation

energies can be explained only in terms of their confinement in the Ge QDs. Figure 3 displays the experimental Raman spectra in the LO region for different laser excitation energies in the $z(yx)z$ scattering geometry. The Raman intensity has a maximum at 2.34 eV, which is close to the resonance corresponding to the E_1 exciton in the Ge QD in [4]. The position of the LO phonons confined in the Ge QD shifts to lower frequencies (by 4–5 cm^{-1}) upon an increase in the excitation energy, which is evidence of the distribution of Ge QDs in size. The Raman intensity for small-sized QDs, in which the E_1 exciton lies at higher energy, increases when the excitation and E_1 energies are at resonance. The optical phonons confined in small-sized QDs are precisely the ones which undergo the largest low-frequency shift. Such a behavior is typical of the Ge-type materials with negative dispersion of optical phonons [14].

In summary, the vibrational spectrum of the Ge/Si superlattices containing Ge quantum dots have been studied in detail. It is found that these structures exhibit properties that are characteristic of both layered structures and quantum dots. The spectrum of acoustic phonons is adequately described by the dielectric continuum model. The low-frequency emission observed in the Raman spectra is caused by the contribution from the phonon states corresponding to the entire acoustic branch because of the violation of translational symmetry in the structures with QDs. As the laser excitation energy increases, the QD-size-selective resonant Raman spectra show a low-frequency shift for the optical phonons confined in the Ge QDs.

This work was supported in part by the Russian Foundation for Basic Research, project no. 00-02-18012.

REFERENCES

1. R. Schrorer, G. Abstreiter, H. Kibbel, *et al.*, Phys. Rev. B **50**, 18211 (1994).
2. S. de Gironcoli, E. Molinari, R. Schrorer, *et al.*, Phys. Rev. B **48**, 8959 (1993).
3. D. J. Lockwood, M. W. C. Dharma-wardana, J.-M. Baribeau, *et al.*, Phys. Rev. B **35**, 2243 (1987).
4. S. H. Kwok, P. Y. Yu, C. H. Tung, *et al.*, Phys. Rev. B **59**, 4980 (1999).
5. J. L. Liu, G. Jin, Y. S. Tang, *et al.*, Appl. Phys. Lett. **76**, 586 (2000).
6. O. P. Pchelyakov, Yu. B. Bolkhovityanov, A. V. Dvurechenskii, *et al.*, Fiz. Tekh. Poluprovodn. (St. Petersburg) **34**, 1281 (2000) [Semiconductors **34**, 1229 (2000)].
7. A. B. Talochkin, V. A. Markov, S. P. Suprun, and A. I. Nikiforov, Pis'ma Zh. Éksp. Teor. Fiz. **64**, 203 (1996) [JETP Lett. **64**, 219 (1996)].
8. A. Milekhin, N. Stepina, A. Yakimov, *et al.*, Eur. Phys. J. B **16**, 355 (2000).
9. A. I. Yakimov, A. V. Dvurechenskii, Yu. Yu. Proskuryakov, *et al.*, Appl. Phys. Lett. **75**, 1413 (1999).
10. S. M. Rytov, Akust. Zh. **2**, 71 (1956) [Sov. Phys. Acoust. **2**, 68 (1956)].
11. T. Ruf, V. I. Belitsky, J. Spitzer, *et al.*, Phys. Rev. Lett. **71**, 3035 (1993).
12. A. Mlayah, A. Sayari, R. Grac, *et al.*, Phys. Rev. B **56**, 1486 (1997).
13. F. Cerdeira, C. J. Buchenauer, F. H. Pollak, *et al.*, Phys. Rev. B **5**, 580 (1972).
14. C. Trallero-Giner, A. Debernardi, M. Cardona, *et al.*, Phys. Rev. B **57**, 4664 (1998).

Translated by V. Sakun